ELECTRICALLY OPTIMIZED MODULE CONCEPTS TO COMPENSATE FAST PERIODIC SHADING SITUATIONS BY MEANS OF PASSIVE ELEMENTS

Hamed Hanifi[1,2]*, Christoph Reyhe[1,2], Bengt Jaeckel[1,2], Jens Schneider[1]
[1]Fraunhofer-Center for Silicon Photovoltaics CSP, 06120 Halle (Saale), Germany
[2]Fraunhofer Institute for Microstructure of Materials and Systems IMWS, 06120, Halle (Saale), Germany
*Corresponding author: +49 345 5589 5515, hamed.hanifi@csp.fraunhofer.de

ABSTRACT: Besides common installation of PV systems, more technical complex applications such as vehicle integrated PV modules or Energy Parks (combined solar and wind farms) gain significant market attraction. One of challenges for such applications is fast periodic shadings by obstacles or wind blades. This paper investigates an approach to integrate passive elements in parallel to each individual cell of the module and compares the performance of a standard PV module with a module with integrated capacitors as passive elements and a PV module with bypass diodes for every single cell under fast periodic shading conditions. For this purpose, in the first step, the module is simulated under different moving shading conditions. In the next step a PV module with open terminals for every solar cell is fabricated and measured outdoor as reference module with no attached elements and with bypass diodes or capacitors for cells under partial shading conditions. The results show that modules with additional capacitors or diodes in module level can benefit higher energy yield compared to standard PV modules. The energy performance of a capacitor integrated module is mainly dependent by the shading transient, due to the time dependent compensating currents of the capacitors. This paper proves the concept of functionality of capacitor for compensation of power loss under shading conditions but the feasibility of integration is a challenge. However, the results show a better performance of the module with bypass diodes compared to the capacitor integrated module with 44 mF capacity.

Keywords: Fast periodic shading, Partial shading, Capacitor, Passive Elements, Bypass diodes

1 INTRODUCTION

Increasing profitability of solar systems is one of the challenges on the way to a successful energy revolution. Besides common installation of solar panels the photovoltaic technology will face new fields of application. Conceivable examples are integrated PV modules on the roof top of trucks and caravans, solar powered trains or hybrid solar-wind parks [1, 2]. Such new areas for use place new requirements on module design and structure, due to inhomogeneous illumination conditions. This paper investigates new module designs where PV modules are frequently affected by fast periodic partial shading.

Considering standard PV modules, all cells are connected in series to match the power requirements in terms of voltage and current. Partial shadings by predictable or unpredictable sources can lead to significant yield loss in PV modules. Furthermore, during partial shading situations, the string operates under negative voltage and the reverse current flow might lead to hot spot problems [3]. Using a diode per string to bypass the current and avoid hot spots is the common solution.

The purpose of this paper is to simulate and determine the influence of quick partial shadings on the energy yield of PV modules. Integration of capacitors and additional diodes to compensate the energy loss under fast periodic shading conditions are analyzed by means of simulation and experiment. To evaluate the performance of the system, all components are modelled and a quick shading concept is defined. Finally, by means of experiment, the trend of simulation results are verified.

2 MODELLING AND SIMULATION

A. Module design

The simulation model is developed based on the two diode model with effective resistors [4, 5, 6]. The solar cells were previously characterized sun simulator to determine the electrical properties. The considered 60-cell module is connected in series to a power supply, which generates a constant current to simulate the current flow from other modules in the array to the module. This current value is equivalent to the current at maximum power point current of the module. With this simplified interconnection, an array with indefinite series connected modules is simulated. The design of the module is shown in Figure 1.

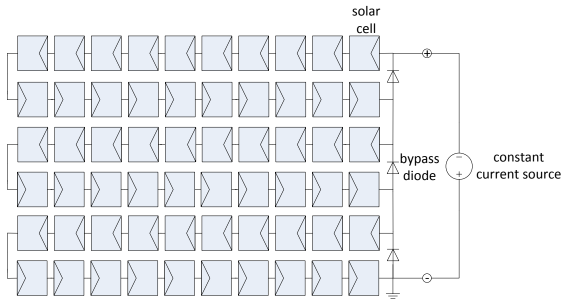

Figure 1: Structure of the PV module model connected in series to a power supply which represents the current flow of the array.

In the further approaches, either a bipolar capacitor or a bypass diode is connected in parallel with reverse polarity to each cell. Since the voltage of the solar cell in reverse bias is negative, it is necessary to use bipolar capacitors to avoid possible damages. The extended equivalent circuit for each cell is shown in Figure 2.

The capacitor supposed to balance the voltage-drop of the respective solar cell by discharging stored energy during partial shading. The capacitor needs to recharge energy, as soon as the corresponding cell generates energy again. On the other hand, the diode supposed to bypass the current of the shaded cell.

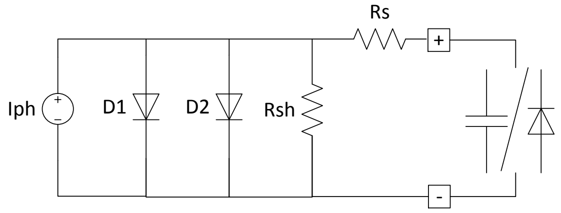

Figure 2: Extended equivalent circuit solar cell with either diode or capacitor connected in reverse parallel.

B. Simulation scenarios

The simulation analyzes and compares the performances of the reference module with no capacitors and three bypass diodes with two modified module designs with either additional capacitors or diodes.

The considered module designs are simulated under the influence of several predefined shading scenarios. As a practical reference, the shading effects which can occur in hybrid solar wind parks are investigated. The constant speed of the partial fast periodic shade is defined with 34 m/s, which corresponds to common nominal speed of wind blades. Furthermore, the shade has an infinite length and a variable width. The width steps are in the scale of the width of a standard solar cell. The roaming shade can pass over the module from various directions. This paper considers two border cases of horizontal and vertical shadings over the module. Besides shading speed, shading direction and shading width, the shading scenario is characterized by the shading intensity, which describes the ratio between minimum photocurrent of the shaded cells and photocurrent of the unshaded cells. The dissipation factor of radiation energy caused by the shading scenario can be described by taking shading width and shading intensity into account. This is defined as "degree of shading" in the further progress of this paper.

$$\text{Degree of Shading} = \frac{\text{shaded area}}{\text{active area module}} \cdot \left(1 - \frac{I_{\text{ph\_min}}}{I_{\text{ph\_max}}}\right) \qquad (1)$$

3 EXPERIMENT

For model validation, an experimental setup, consisting of standard 60-cell PV module, power supply, oscilloscope, power resistor, two capacitor banks and two bypass diodes per solar cells under shading conditions and a shading system are designed. The PV module has the capability to interconnect electronic elements at the terminals of each individual cell. In the next step, the module is measured in outdoor conditions with known environmental parameters. The capacitance of the capacitor banks can be adjusted between 11, 22 and 44 mF. The diodes are commonly used bypass diodes for PV applications. The shading system is mounted on the edge of the module and can frequently partially shade two solar cells. The shading system consists of a black paper board which rotates around its vertical axis and is mounted on the rotor shaft of a direct current motor (see Figure 3). The maximum shaded area of one cell is 44 percent as it is shown in Figure 3. The motor rotates with a constant frequency of 2 hertz. To have the worst case scenario, the shading blade is mounted in a way to shade two cells each located in different string. The rotor blade has a circular shape at the top and a rectangular shape at the bottom. This shape casts the biggest possible shade over the two cells without directly affecting the cells beside (see Figure 4).

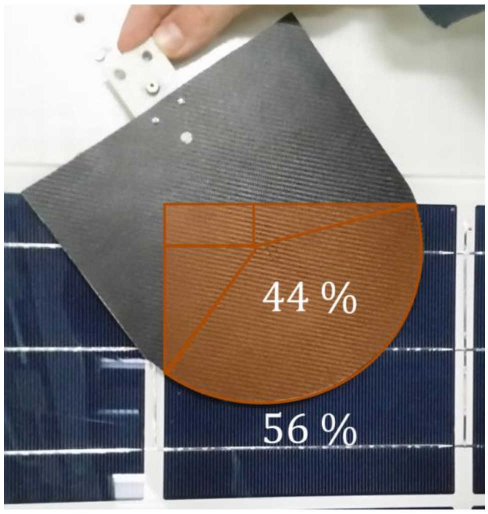

Figure 3: Shading system covers 44 percent of solar cell area in the worst position.

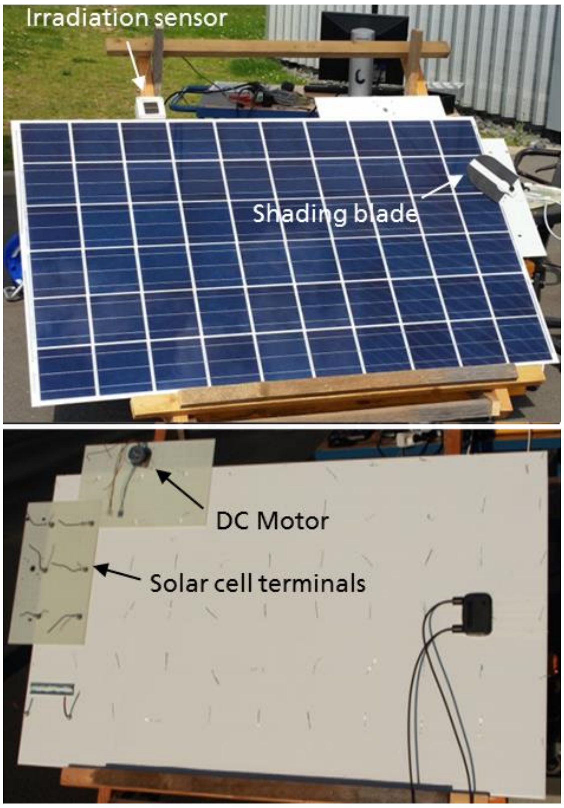

Figure 4: Front (top) and rear (bottom) side of the designed module with possibility of connection of capacitors or diodes at the terminals of each individual cell. The module is mounted in an angle of 45° and the shading system partial shades two cells of two different strings on the right side.

The power supply is connected in series to the module and works as a constant current source by generating the current at maximum power point of the reference module. This value is measured with a peak power measuring device, including an external irradiation sensor at the beginning of the experiment. The power resistor has a resistance of 10 Ω and is connected in series to the module and the power supply to consume the generated energy of the module and the power supply. An oscilloscope is connected at the terminals of the module and records the module voltage and current over the time. The equivalent circuit of the experimental setup is shown in Figure 5.

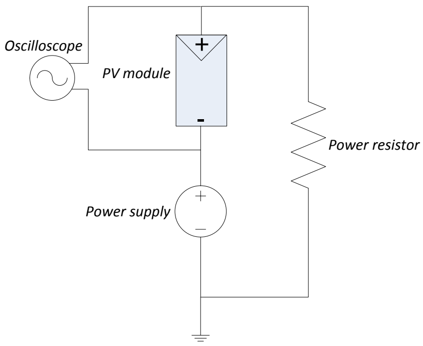

Figure 5: Equivalent circuit of the experimental setup.

4 RESULTS AND DISCUSSION

A. *Simulation – capacitor integrated module*

The simulation results show that the module performance is affected by shading direction, shading width and shading intensity. The highest impact on the module performance is the shading direction.

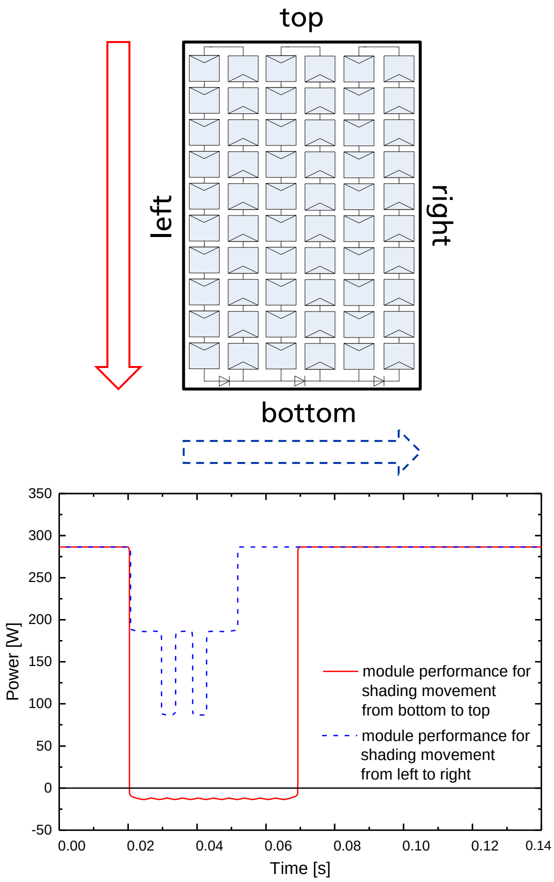

Figure 6: Common interconnection concept of a full cell module (top); and module performance under moving partial shading conditions from bottom to top and left to right directions (bottom).

The common electrical design of full cell modules consists of 60 cells, which are connected in series in longitudinal direction of the module. The cells are divided into 3 strings connected in parallel to one bypass diode. Figure 6 shows the module design of a 60 cell module and the different module performances for two considered shading directions. In this example the width of the shade is equal to the width of the cells.

Due to the interconnection design of the reference module, all three strings are affected simultaneous, when the shade hits the module from bottom to top. All three diodes conduct during the partial shading resulting negative module voltage. The negative power of the module represents the power consumption by the diodes.

When the roaming shade passes over the module from left to right, the strings are affected one after the other. This leads to the power of almost one-third of the module power during the shading. The worst case situation happens when the shade pass through one string to another and affect two strings for a short time. In this case, the module loses two strings but produce at least one-third of the power during partial shading. The duration of partial shading between the two considered scenarios varies due to the rectangular profile of the module.

Figure 7 shows two diagrams with the power curves of the reference PV module and the capacitor integrated module with an exemplary capacitance per cell of 50 mF. In both cases, the module is affected by the same fast periodic partial shade which is already described in Figure 6. Area A represents the energy loss of the reference module under partial shading condition. The energy compensation due to the compensating currents of the capacitors during shading period is pictured with area B. Area C represents the energy losses due to capacitors recharge process. In order to evaluate the results, the energy compensation is calculated by equation (2).

$$Energy\ compensation = \frac{B - C}{A} \tag{2}$$

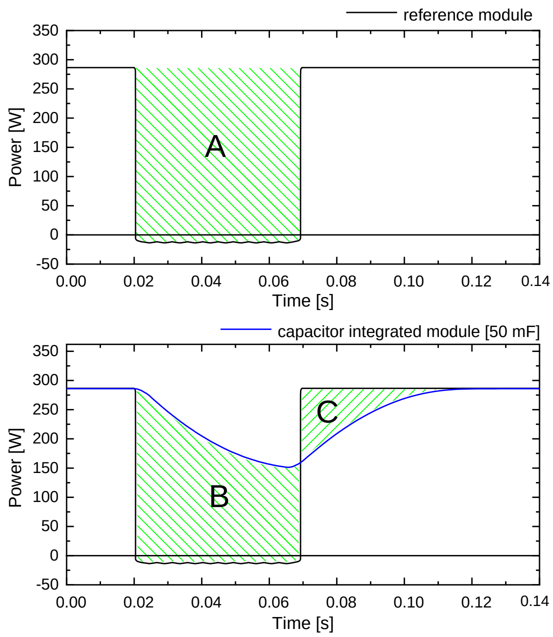

Figure 7: Simulated energy curves of the reference PV module and the capacitor integrated module.

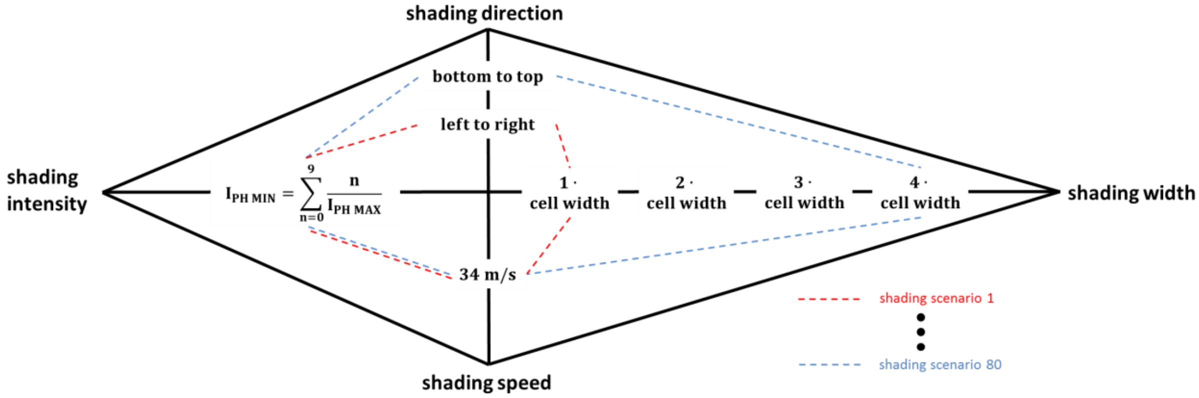

Figure 9: Variation in shading parameters results in 80 different considered shading scenarios

When the energy compensation is 1 all losses are recovered.

Figure 8 shows the time sequences of the module power with capacitive current compensation for different capacity values and two shading movement scenarios. The shade characteristic remains as what was previously described. The energy compensation increases with higher capacitance. The energy compensation for left to right shading scenario is better than bottom to top scenario for similar capacity values. The reason of better compensation lays over the shading profile which gives more time to capacitors to recharge and shorter discharge time over the power loss due to the shading.

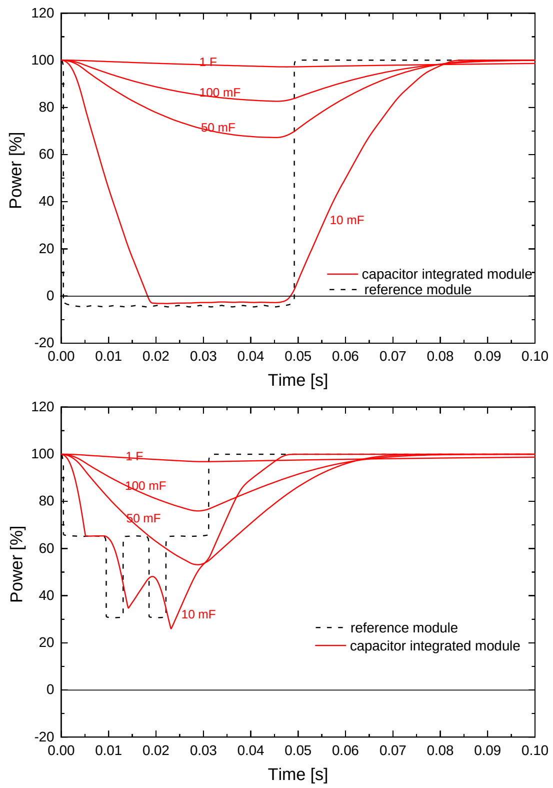

Figure 8: Time sequences of the module power with capacitive compensation currents for different capacity values. Partial shade hits the module from (top) bottom to top and from left to right in the bottom diagram.

In order to analyze the energy performance for a randomized shading characteristic, 80 different shading scenarios are simulated. Figure 9 shows the respective composition of parameters:

- shading speed
- shading direction
- shading width
- shading intensity

Those shading scenarios were simulated for 5 different capacitor integrated modules. For each module the capacitance of the integrated capacitors is always 10 mF, 50 mF, 100 mF, 500 mF or 1 F. Figure 10 illustrates the average energy compensation compared to the reference module over all shading scenarios in accordance to the capacitor integrated module. This diagram allows a qualitative statement about the energy performance of the capacitor integrated modules compared to the reference module. The simulation results show that the capacitance for each cell needs to be at least in a millifarad scale to have a positive impact on the energy performance during the partial shading situation. Smaller capacitances can even lead to worse performance compared to reference module.

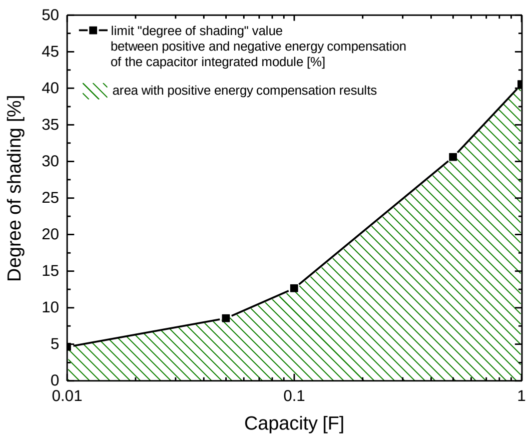

Figure 10: Average energy compensation over all shading scenarios in accordance to the capacitor integrated module

B. Simulation – diode integrated module

The second approach for shading resistant module design is the integration of bypass diodes for each single solar cell. Figure 12 shows the energy yield for 3 considered modules: reference module, schottky diode integrated module (with forward bias voltage of 0.3 V) and silicon rectifier diode integrated module (with forward bias voltage of 0.7 V). Partial shade hits the module from bottom to top and shade width is equal to cell width and shading intensity is 50 %.

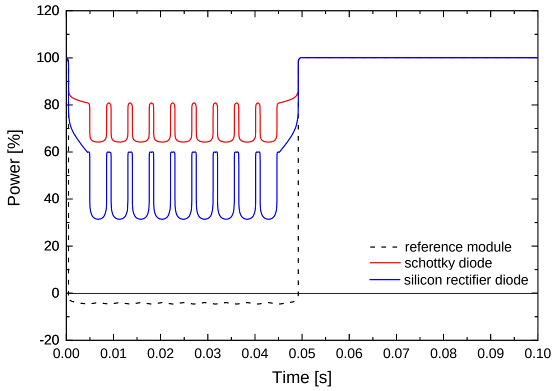

Figure 11: Output power of the reference module, schottky diode integrated module and silicon rectifier diode integrated module. Partial shade hits the module from bottom to top and shade width is equal to cell width and shading intensity is 50%.

The results show that the diode integrated module concept is able to some extent bypass the energy loss. The quality of energy compensation is dependent on the type of the diode. Schottky diodes are more suitable compared to standard silicon rectifier diodes due to the smaller forward voltage characteristic. Figure 12 displays the energy compensation (compared to the reference module) for both capacitor integrated and diode integrated modules. The switching characteristic of diodes is time independent in comparison to the charge and recharge characteristic of capacitors. The energy compensation of diode integrated modules is more static in accordance to shading period. Using schottky diodes instead of silicon rectifier diodes results in about twice more energy compensation values.

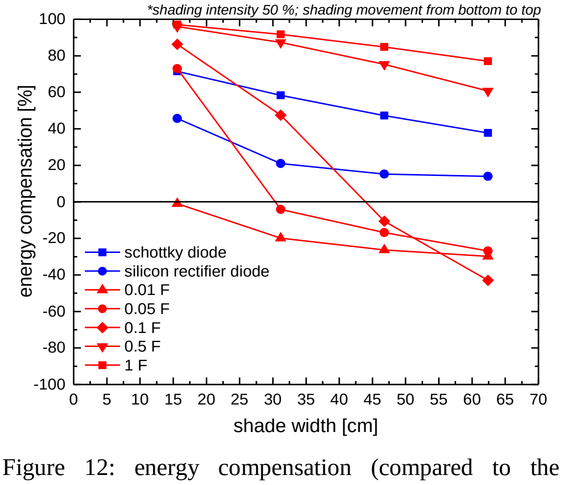

Figure 12: energy compensation (compared to the reference module) of the capacitor and the diode integrated modules in respect to the shade width.

C. Experiment

To prove the concept, the PV module is measured in outdoor under light intensity of 671 W/m^2. Since the whole experiment takes place less than two minutes, the deviation of light intensity is negligible. In the beginning, the module is measured under no shade condition. In the next step, the shading object started to shade two solar cells periodically. Finally, the capacitors with the capacity of 44 mF are connected to the module and the performance is measured under the shading conditions. Figure 13 demonstrates the performance of the PV module without and under shading conditions with and without integration of capacitors. The results prove the concept and trend matches with simulation results.

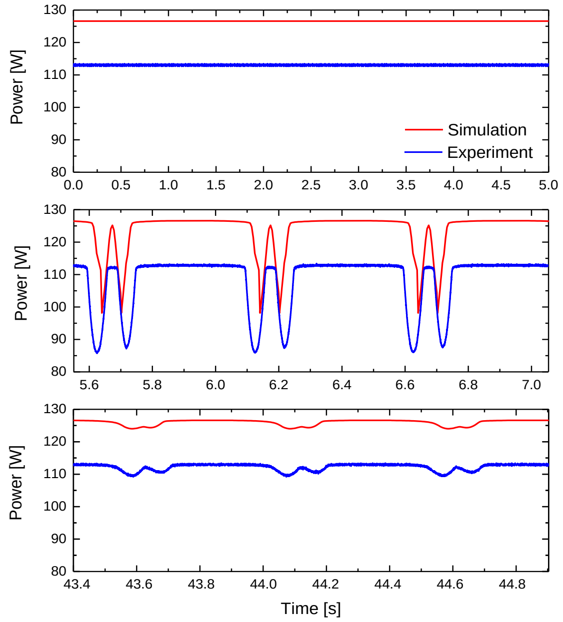

Figure 13: Measurement and simulation results of the module without shading (top diagram), under periodic shading conditions of two solar cells without capacitors (middle) and under periodic shading conditions of two solar cells each connected to a capacitor bank of 44 mF (bottom). The process is sequential and takes place within every 46 seconds. The irradiation intensity is 671 W/m^2. The difference between the simulation and measurement results comes from the neglecting of electrical losses in interconnection in simulation and sharp tilt angle of the module in the experiment.

Figure 14 show the experimental and simulated energy performance of the reference module and the capacitor integrated module with 11 mF, 22 mF or 44 mF capacities respectively. Figure 15 shows the experimental and simulated energy performance of the reference module and the diode integrated module with common used silicon rectifier bypass diodes. The shading system partially shades two cells of the module during the shading periods. Generally, it should be noted that the average output power of the simulated module is higher than in the experimental setup due to the neglecting of electrical losses in interconnections and optical losses (reflection and sharp tilt angle). The partial shading of the two cells results in a power drop of the module in studied cases. The slight delay in measurement results can be expressed by considering the power supply characteristics. In the simulation, the power supply is classified as ideal. However, in the experimental setup, the behavior of the power supply is based on an internal regulated circuit. It can be assumed that the simulation model is reasonable and the simulated results comply with the practical results. The comparison in this chapter can be seen as a plausibility check for both simulation model and experimental results.

Comparison of the energy compensation between different capacitors demonstrates a positive compensation for capacities above 22 mF. The energy compensation for the capacitor with 44 mF reaches up to 58% in experiment and 79% in simulation (due to the offset in power). Comparing the module with 44 mF capacitor and the module with bypass diodes shows 33% more compensation for the measured diode integrated module compared to the capacitor integrated version.

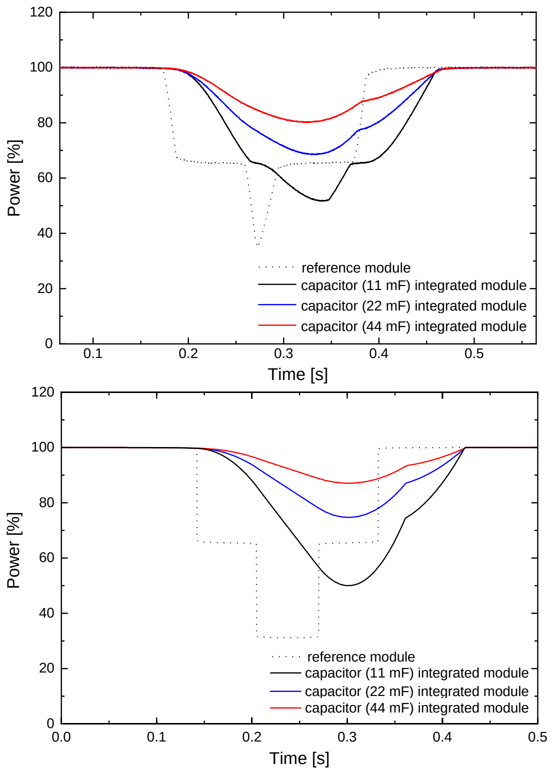

Figure 14: Experimental (top diagram) and simulated (bottom diagram) module performance during partial shading of two cells. Pictured are the energy curve of the reference module and the capacitor integrated modules.

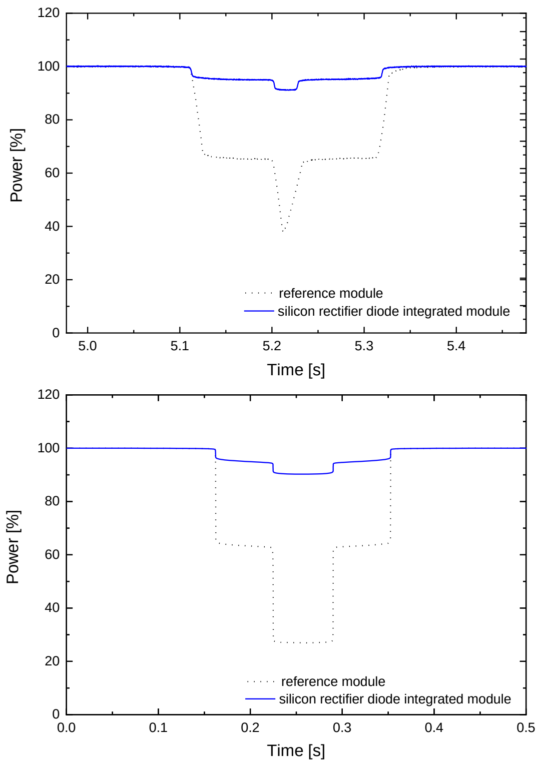

Figure 15: Experimental (top diagram) and simulated (bottom diagram) module performance during partial shading of two cells. Pictured are the energy curve of the reference module and the diode integrated modules.

5 CONCLUSION AND OUTLOOK

The results show that the capacitor and diode integrated modules are less sensitive to periodic fast partial shading than common standard modules. The performance of capacitor integrated modules is highly dependent on the considered shading frequency due to the exponential conducting currents.

By taking the defined shading scenarios into account, the capacity of each cell needs to be at least in millifarad scale depending on the current level to reach a positive impact on the module performance.

Diode integrated modules are nearly frequency independent due to the short switching characteristic of diodes. By using schottky diodes with a forward voltage of about 0.3 V instead of silicon rectifier diodes with a forward voltage of about 0.7 V, it almost doubles the energy compensation effect of the module.

The technical and economic realization of PV modules with interconnected capacitors is not feasible, yet. With today's technology, the integration of the required capacity sizes is expensive and requires a lot of work to be implemented. The best conceivable solution for the future would be the integration of technically improved capacitors as an additional layer in PV modules, as shown in Figure 16.

In collaboration with the Interdisciplinary Center for Material Sciences at Martin Luther University Halle-Wittenberg in Germany, a film capacitor was developed and interconnected to the module circuit before lamination. The bodies of solar cell and capacitor were isolated by polymer films. Due to the individual characteristic of film capacitors, the achievable capacitance is in the range of a few nanofarad. Hence, the approach to directly integrate capacitors in the module structure is not yet feasible and extra work on development of new films is required. The integration of bypass diodes for each cell requires less work to be implemented. The temperature dependent behavior, as well as the charge cycles of the capacitors, were excluded in this paper and require further research investigations. In order to develop electrically optimized module concepts for applications with high shading fluctuation, other aspects need to be considered.

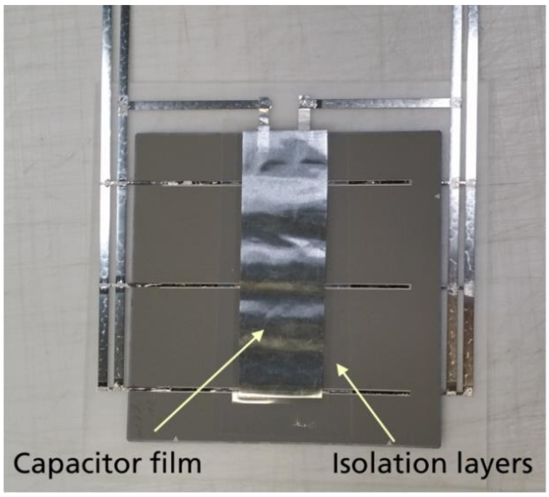

Figure 16: Rear side of a solar cell with a parallel connected film capacitor before lamination.

ACKNOWLEDGEMENTS

The authors thank Till Maelzer from the Interdisciplinary Center for Material Sciences at Martin Luther University Halle-Wittenberg for providing the capacitor film for testing.

6 REFERENCES

[1] S. Schindler, D. Götz und J. Schneider, „Beyond Watt per Module and Costs per Watt – New Weight Related Parameters for Photovoltaic Modules," in *35th European Photovoltaic Solar Energy Conference and Exhibition*, Brussels, 2018.

[2] M. S. Vasisht, G. Vashista, J. Srinivasan und S. K. Ramasesha, „Rail coaches with rooftop solar photovoltaic systems: A feasibility study," *Energy*, Bd. 118, pp. 684-691, 2017.

[3] S. Ahsan, K. A. K. Niazi, H. Khan und Y. Yang, „Hotspots and performance evaluation of crystalline-silicon and thin-film photovoltaic modules," *Microelectronics Reliability*, pp. 1014-1018, 2018.

[4] H. Hanifi, J. Schneider und J. Bagdahn, „Reduced shading effect on half-cell modules-measurement and simulation," in *32st European Photovoltaic Solar Energy Conference and Exhibition*, Hamburg, 2015.

[5] S. Guo, J. Schneider, F. Lu, H. Hanifi, M. Turek, M. Dyrba und I. M. Peters, „Investigation of the short-circuit current increase for PV modules using halved silicon wafer solar cells," *Solar Energy Materials & Solar Cells*, Bd. 133, pp. 240-247, 2014.

[6] H. Hanifi, D. Dassler, J. Schneider, M. Turek, S. Schindler und J. Bagdahn, „Optimized tab width in half-cell modules," *Energy Procedia*, Bd. 92, pp. 52-59, 2016.